

Cardiac Mechanics Evaluated by Speckle Tracking Echocardiography

Maria Cristina Donadio Abduch¹, Adriano Mesquita Alencar², Wilson Mathias Jr.¹, Marcelo Luiz de Campos Vieira^{1,3}

Instituto do Coração, Faculdade de Medicina da Universidade de São Paulo¹, São Paulo, SP; Instituto de Física, Universidade de São Paulo², São Paulo, SP; Hospital Israelita Albert Einstein³, São Paulo, SP - Brazil

Abstract

Natural myocardial markers, or speckles, originated from constructive and destructive interference of ultrasound in the tissues may provide early diagnosis of myocardial changes and be used in the prediction of some cardiac events. Due to its relatively temporal stability, speckles can be tracked by dedicated software along the cardiac cycle, enabling the analysis of the systolic and diastolic function. They are identified by either conventional 2D grey scale and by 3D echo, conferring independence of the insonation angle, thus allowing assessment of cardiac mechanics in the three spatial planes: longitudinal, circumferential, and radial. The purposes of the present paper are: to discuss the role and the meaning of cardiac strain obtained by speckle tracking during the evaluation of cardiac physiology and to discuss clinical applications of this novel echocardiographic technology.

Introduction

Speckles are originated from the constructive and destructive interference of insonation in tissues. Numerous of these small grey-scale spots, which measures less than an ultrasound wavelength, are clustered in regions of interest with approximately 20-40 pixels, called kernels. Kernels are supposed to be relatively stable in time, exhibiting a specific pattern, like a "fingerprint", that can be tracked by dedicated software along the cardiac cycle, by the sum of absolute difference specific algorithms (Figure 1)¹.

Twenty two years after having been considered "an undesirable property of the image as it masks small differences in grey level"², speckles started to be employed as myocardial natural markers, capable of evaluation and quantification of the cardiac function in a reproducible, accurate and simple way. This new use has improved the understanding of cardiac mechanics, enabling early detection of changes in heart performance and, as a consequence, promoting more effective therapeutic approaches.

This paper aims to compile the core information on cardiac mechanics evaluated by speckle tracking echocardiography

Keywords

Echocardiography / methods; Strain, torsion, speckle tracking; Heart Diseases.

Mailing Address: Maria Cristina Donadio Abduch •

Praça Guido Cagnacci, 05, Vila Madalena. Postal Code 05444-060, São Paulo, SP - Brazil

E-mail: cristinaabduch@cardiol.br, abduchmc@gmail.com

Manuscript received April 29, 2013, revised manuscript October 14, 2013, accepted October 16, 2013.

DOI: 10.5935/abc.20140041

(STE), providing a broad view about the basic principles and clinical applications of this novel technology.

Strain and Strain Rate – Basic Principles

Considering a given one-dimensional object under either lengthening or shortening deformation, so that the initial length is L_0 and its length in a given time is $L(t)$. The normalized deformation, strain ε , can be mathematically represented by the following equation:

$$\varepsilon(t) = \frac{L(t) - L_0}{L_0} \quad (1)$$

This is the Lagrangian strain, which occurs when the initial length is known. However, whenever the original length is unknown, strain can be assessed considering its small temporal variations $d\varepsilon_N(t)$ during an infinitesimal time increment dt , as mathematically translated by the equation below:

$$d\varepsilon_N(t) = \frac{L(t+dt) - L(t)}{L(t)} \quad (2)$$

Where $L(t+dt)$ is the lengthening at the first next infinitesimal time interval considered, after the time t .

The sum of all strain changes in different infinitesimal time intervals provides the total strain, and if the dt is small enough the sum become an integral over $d\varepsilon$, or

$$\varepsilon_N(t) = \int_{t_0}^t d\varepsilon_N(t') \quad (3)$$

This is the natural strain and represents variations during the total process of shortening or lengthening. Regarding small changes, Lagrangian and natural strain share almost the same values. Nevertheless, considering the large cardiac deformations that occur during systole and diastole, natural strain seems to be of more appropriate to use, since the original length is not known³.

Strain is a dimensionless measurement of changes in shape, hence, deformation. Variations in shortening or lengthening occur only under differences in velocities; without this prerequisite, what is observed is only movement from one point to another, without deformation. Strain rate (SR) is the velocity of deformation, expressed as s^{-1} and represents the average deformation in a given time interval. A SR of $0.8 s^{-1}$ means that the object deforms, in average, 80% during one second³.

Considering a two-dimensional object, two types of strain can take place: normal strain, which happens along the x and y axes and shear strain, occurring in a perpendicular spatial way taking into consideration two parallel planes. Three-dimensional objects are submitted to three normal strains (x , y and z axis) and six shear strains combining different spatial planes (xy , xz , yx , yz , zx and zy)³.

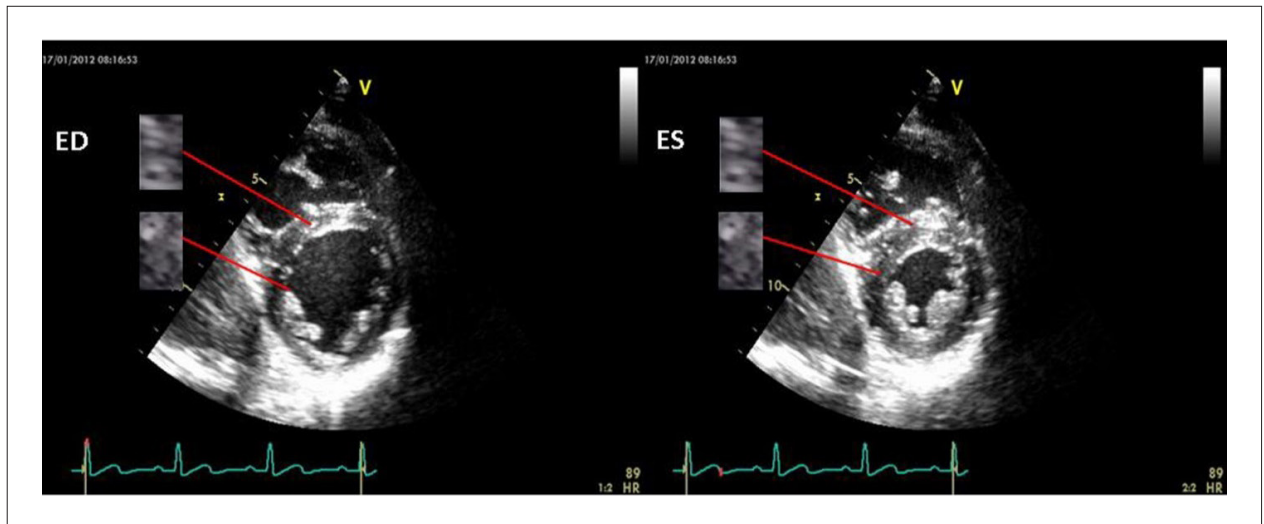


Figure 1 - Regions of interest (kernels) represented in the end-diastole (ED) and end-systole (ES). Note the speckle tracking fingerprint pattern of each one, which is constant along the cardiac cycle.

Myocardial Strain Evaluated by Speckle Tracking Echo

Speckle tracking allows appraisal of strain and SR using the conventional 2D echo grey scale, thus enabling the assessment of deformation in the longitudinal, circumferential and radial planes, since there is no dependence on the insonation angle¹. Transmural, subendocardial and subepicardial strains can be obtained. It is well established that, once wall stress is greater in subendocardial layer, this region sustains higher deformational changes than the subepicardium during systole, leading to higher myocardial pressure and oxygen demand⁴.

Radial systolic strain is positive, since it represents myocardial thickening (the final length is greater than the initial one) – Figure 2A. On the other hand, longitudinal and circumferential strains have negative values, since the initial length is higher than the final one (Figures 2B and 2C).

Myocardial strain evaluated by STE showed good correlation either in experimental models, when compared with sonomicrometry as the gold standard, as well as in initial clinical trials enrolling patients with myocardial infarction, comparing this novel technology with well-established echocardiographic techniques, such as Doppler Tissue Imaging (DTI) and wall motion score index^{1,5}.

Myocardial deformation is affected by load conditions: strain is more vulnerable, correlating more with left ventricular ejection fraction; SR is less influenced, being strongly related to left ventricular contractility⁶. Additionally, strain and SR are predisposed to gender and age related changes⁷.

Left Ventricular Rotation, Twist and Torsion

Torsion is a complex process of the cardiac mechanics, involving deformation both in circumferential and longitudinal planes given by the obliquely arranged subendocardial and subepicardial fibers disposed, respectively, in a right and left handed orientation, and interacting with each other in order

to promote the left ventricular (LV) twist. The latter, when analyzed from the cardiac apex, occurs through the opposite apical counterclockwise and basal clockwise rotation, measured as the difference between these angles (θ_{ap} and θ_b , respectively). Torsion is analyzed as the twist divided by the LV length (h) in the longitudinal plane, thus expressing the twist considering the distance observed between the left ventricular apical and basal slices. Torsion in relation to the mean epicardial apical and basal radii (ρ_{ap} and ρ_b , respectively) is the torsional shear angle T , as calculated according to⁸:

$$T = \frac{(\theta_{ap} - \theta_b) \times (\rho_{ap} + \rho_b)}{2h} \quad (4)$$

The torsional shear angle allows comparisons between hearts of different sizes, since the cardiac twist is qualitatively equivalent in man and mice, differing in magnitude according to the heart size. Therefore, torsion has been quantitatively comparable in both species, despite the discrepant size of the hearts⁹.

After magnetic resonance (MRI) convention, STE basal rotation values are settled as negatives, once the apical ones are established as positives. Considering the larger epicardial lever arm and the higher apical rotation values, in normal conditions, twist and torsion are positive¹⁰.

Studies have demonstrated that torsional mechanics assessed by STE has a good correlation with sonomicrometry, and with methods that present both good spatial (MRI) as well as temporal (DTI) resolution^{11,12}.

Torsion, measured as the net twist divided by LV length, increases with age¹³: during infancy and childhood, both LV base and apex rotate counterclockwise; gradually, between 5 to 10 years old, the base starts changing its rotation pattern to clockwise, and this is completely consolidated by the adolescence. From adulthood to middle-age and older, the enhancement in twist is due to increased counterclockwise apical rotation. Torsional mechanics is also affected by loading

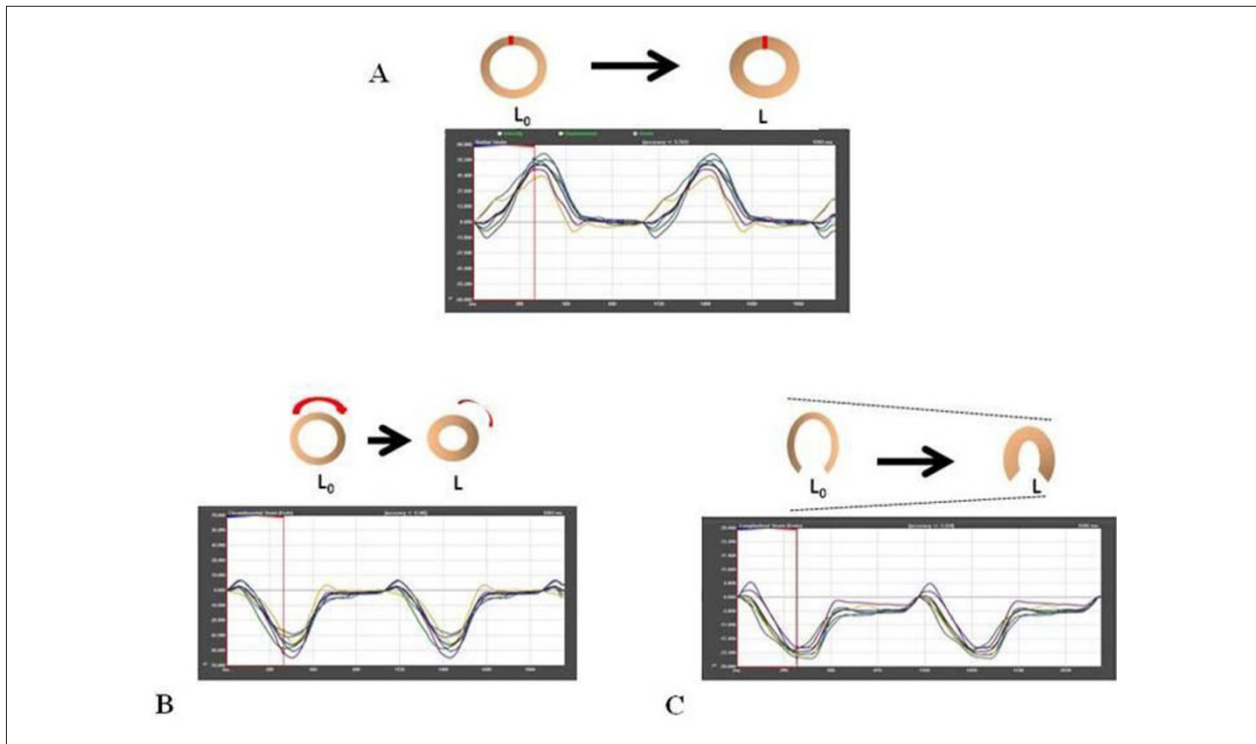


Figure 2 - Strain curves in the radial (A), circumferential (B) and longitudinal (C) planes. Note that, considering the radial strain, L_0 is smaller than L , resulting in positive strain curves; otherwise, regarding the circumferential and longitudinal strains, L_0 is higher than L , originating negative curves. Each segment of the left ventricle is identified by a different color that varies according to dedicated software.

conditions and inotropic state, increasing with higher preload, decreasing with higher afterload and is proportional to the positive inotropism¹⁴.

Systolic torsion enhances maximum intracavitary pressures with minimum fiber shortening, resulting in less oxygen demand⁸.

Recoil occurs at the beginning of ventricular repolarization, when the subendocardial apex undergoes relaxation and returns to its original position by reversal of systolic counterclockwise rotation. Apical recoil results from the release of restoring forces accumulated with torsion during ventricular ejection; these forces increase the intraventricular pressure gradient that promotes the suction of blood after mitral valve opening, during the early ventricular diastolic filling. As it occurs before mitral valve opening, during the isovolumic relaxation period, it represents a link between systole and diastole, and is less influenced by load conditions. Additionally, it is proven that apical recoil correlates well with τ , the time constant of LV pressure decay¹⁵. Assays have also showed the relevance of the recoil to evaluate the ventricular diastolic function¹⁶.

Normal values

The normal values obtained by STE are listed in Table 1; the wide range of variation is mainly due to different dedicated software (once the values are not interchangeable between different manufacturers) and to the heterogeneity related to age and gender^{311,12,17-22}.

According to the HUNT study⁷, enrolling 1266 healthy individuals, peak systolic global longitudinal strain and SR decreases with age and is lower in men. The average values for longitudinal strain and SR were, respectively: -17.4%, -1.05 s⁻¹ in women and - 15.9%, -1.01 s⁻¹ in men.

Shear Strain

Shear strain is observed when two parallel planes move at different velocities, deforming a cube into a parallelepiped: as the planes slide over each other, deformation occurs at the perpendicular level. When this tangential change in shape takes place, the perpendicular plane rotates at a certain angle – the shear angle. Shear strain is measured like normal strain, but at the perpendicular plane. Considering the heart, there are three types of shear strain: CL (shear in the circumferential and longitudinal planes), CR (shear between the circumferential and radial planes) and RL (shear among radial and longitudinal planes) – Figures 3 to 5. Basically, CR strain means the transmural gradient consequent to the differences between subendocardial and subepicardial deformation, RL strain express thickening and CL strain represents torsion. Subendocardial and subepicardial gradients exert influence in all three shear strains, determining regional myocardial deformation heterogeneity and predicting slide over myocardial fibers: the greater the gradient, the larger the shear strain²³.

Table 1 – Normal values for cardiac mechanics parameters evaluated by speckle tracking

Parameter	Normal Values
	-22.1 ± 2.0
	-22.1 ± 2.1
Global Longitudinal strain (%)	-18.7 ± 2.2
	-19.9 ± 5.3
	-16.7 ± 4.1
Basal Longitudinal strain (%)	-16.2 ± 4.3
Mid-Ventricle Longitudinal strain (%)	-17.3 ± 3.6
Apical Longitudinal strain (%)	-16.4 ± 4.3
	-1.3 ± 0.2
Longitudinal strain rate (s ⁻¹)	-1.45 ± 0.2
	-1.03 ± 0.27
Basal Longitudinal strain rate (s ⁻¹)	-0.99 ± 0.27
Mid-ventricle Longitudinal strain rate (s ⁻¹)	-1.05 ± 0.26
Apical Longitudinal strain rate (s ⁻¹)	-1.04 ± 0.26
	-21.8 ± 4.2
Circumferential strain (%)	-22.1 ± 3.4
	-27.8 ± 6.9
Circumferential strain rate (s ⁻¹)	-1.7 ± 0.2
	59.0 ± 14.0
Radial strain (%)	73.2 ± 10.5
	35.1 ± 11.8
Radial strain rate (s ⁻¹)	2.6 ± 0.6
	-5.8 ± 2.0
Basal rotation (°)	-4.6 ± 1.3
	11.7 ± 3.5
Apical rotation (°)	10.9 ± 3.3
	17.4 ± 3.7
	14.5 ± 3.2
Twist (°)	9.0 ± 2.0
	19.3 ± 7.2
Torsion (°/cm)	2.47 ± 0.94

The heterogeneity in myocardial deformation and the contribution of shear strain to cardiac systolic function was previously demonstrated in dogs²⁴ and in healthy adult humans²⁵.

3D Strain

Maffessanti et al (26) observed that the 3D STE presented higher values for radial displacement and rotation in comparison with 2D STE, indicating the 2D limitation to track the out of plane imaging speckles. Longitudinal displacement was not different between both methods, once in the longitudinal axis the out of plane motion is smaller in relation to the radial one²⁶. The concept of

area tracking, integrating data obtained by longitudinal and circumferential strain, has recently been introduced, aiming at reducing the tracking error. The validation against sonomicrometry showed strong correlations and good reproducibility²⁷.

Clinical trials have demonstrated that 3D STE can be employed for the early detection of cardiac changes, as in familial amyloid polyneuropathy (Figure 6)²⁸, and to fully understand the pathophysiological aspects of the cardiac alterations, as in sickle cell disease²⁹.

Probably, one of the most compelling understandings regarding 3D STE analysis is the single beat image acquisition once it is not based on 2D reconstruction to comprise the full volume, overcoming the issue of low frame rates, arrhythmias, respiratory and patient movement interferences. Hitherto, the first studies using this novel technology to evaluate LV volumes and function have shown good correlations when compared with MRI (*r* values around 0.90)^{30,31}.

Left Atrial Strain

Dedicated software is the same developed originally for LV analysis, leading to certain limitations. However, previously published analyses have encouraged the assessment of this chamber through this novel technology. Since LA is a predictor of cardiovascular events, tools that provide a reliable assessment of this chamber are of utmost relevance³². Some studies showed a close association between LA structure and performance in healthy volunteers, patients with LV heart failure with normal ejection fraction and in individuals with diastolic dysfunction³³. Patients with heart failure and normal LV ejection fraction showed significant reduction in LA longitudinal strain during the early and late LV diastolic filling. Those results indicate subendocardial fiber impairment, as these fibers are arranged mainly in the longitudinal plane in the LA anatomy³⁴.

Clinical Applications

Dilated Cardiomyopathy (DCM)

One of the most relevant applications of STE is the ability to prognosticate patients with DCM. The studies showed cut-off values between -4.9% and -12% for global longitudinal strain³⁵⁻³⁷ in the prediction of events.

Patients may also present rotations in opposite directions compared with the normal population. Probably, this finding may be attributed to the evidence of fibrosis and changes in the myocardial obliquely oriented fibers. In normal individuals, fibers are disposed around 60° in relation to the longitudinal plane; the dilation alters this angle to approximately 90°, in a more transverse direction, affecting the normal characteristics of rotation³⁸.

Hypertrophic Cardiomyopathy (HCM)

This autosomal dominant myocardial disease has various phenotypical expressions, generally with subclinical abnormal diastolic and systolic function³⁹. None of the established

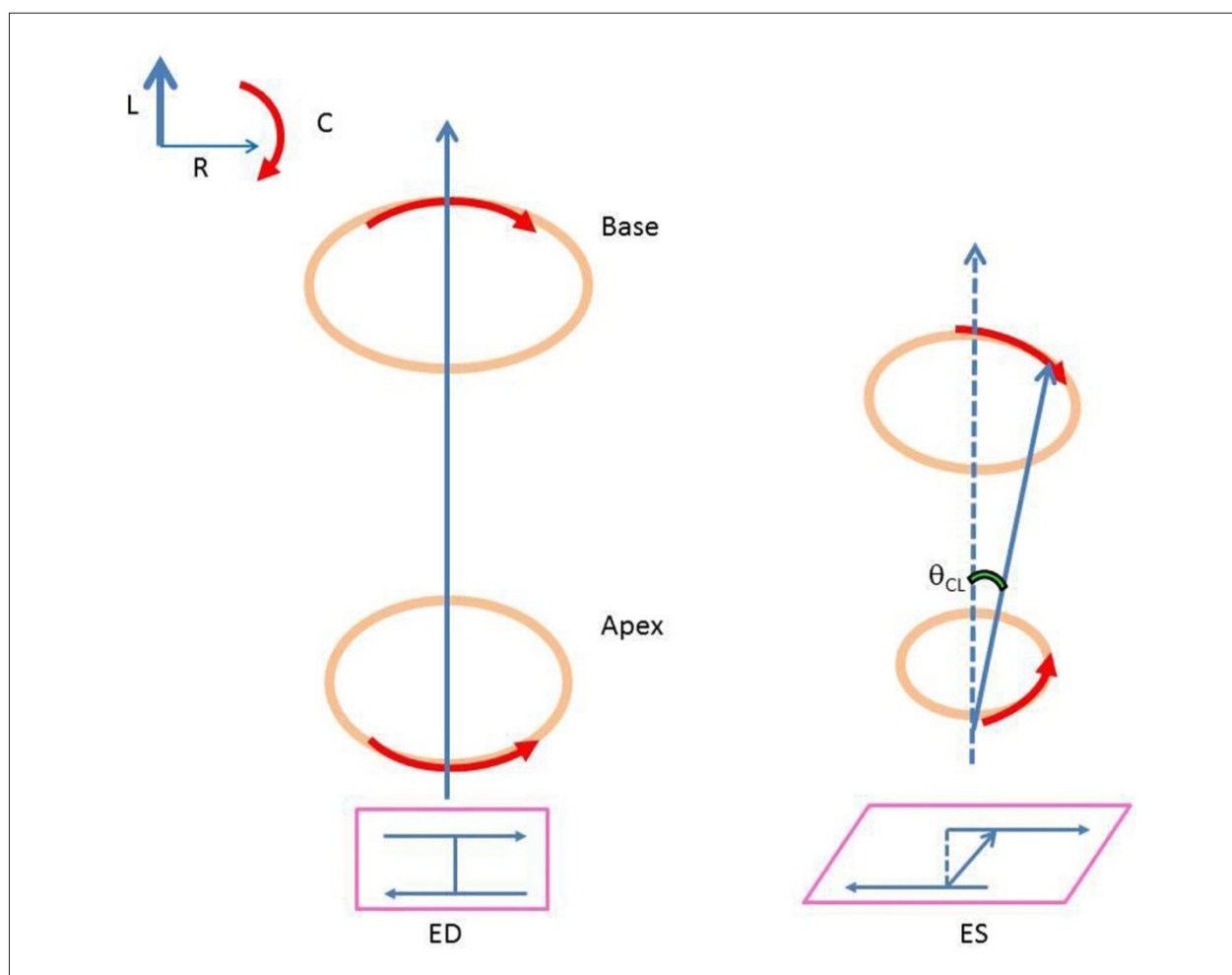


Figure 3 - Circumferential-Longitudinal strain. Top left: the three orthogonal planes (L: longitudinal; C: circumferential; R: radial). The basal slice rotates clockwise and the apical slice counterclockwise, creating two parallel planes moving in opposite directions and originating a deformation at the perpendicular plane (shear strain). The rotation resulted from shear strain is the CL angle, which basically means TORSION. ED: end-diastole; ES: end-systole; θ_{CL} : circumferential-longitudinal strain angle.

echocardiographic parameters are sensitive and specific enough to detect subtle changes or difference between phenotypes; thus, the STE assessment represents a cornerstone in the evaluation of patients with this condition⁴⁰.

Apical rotation and twist showed to be increased in patients with reverse septal curvature in comparison with sigmoidal HCM, probably due to the subendocardial ischemia at the affected region⁴¹; apical recoil in HCM population was delayed when compared with healthy volunteers⁴². The importance of understanding the association between the genotype, phenotype and function is settled in the possibility of categorization of patients into specific clinical subgroups, establishing a less heterogeneous prognosis.

Popovic et al⁴³ showed reduction in the ventricular longitudinal strain even in areas without hypertrophy and Paraskevaidis et al⁴⁰ demonstrated the prognostic value of the LA systolic strain determined by STE in patients with HCM and LV hypertrophy secondary to other causes.

Pericardial Diseases and Restrictive Cardiomyopathy

Undoubtedly, one of the greatest challenges in cardiology is the differential diagnosis between restrictive cardiomyopathy and constrictive pericarditis. TDI analysis provides some possibilities; however, this evaluation basically regards the longitudinal plane⁴⁴.

Longitudinal strain was reduced in patients with restrictive cardiomyopathy, while in those with constrictive pericarditis the changes involved radial and circumferential strain, torsion and apical recoil. Since restrictive cardiomyopathy is characterized by infiltrative deposit and fibrosis, jeopardizing mainly the subendocardium, the longitudinal component of cardiac deformation is the most affected one. Concerning pericardial disease, it can extend to the subepicardial layer, compromising mainly the radial and circumferential constituents of cardiac mechanics⁴⁵.

Coronary Artery Disease and Myocardial Infarction

Speckle tracking is emerging as a useful tool in the assessment of viable myocardium, by providing a regional

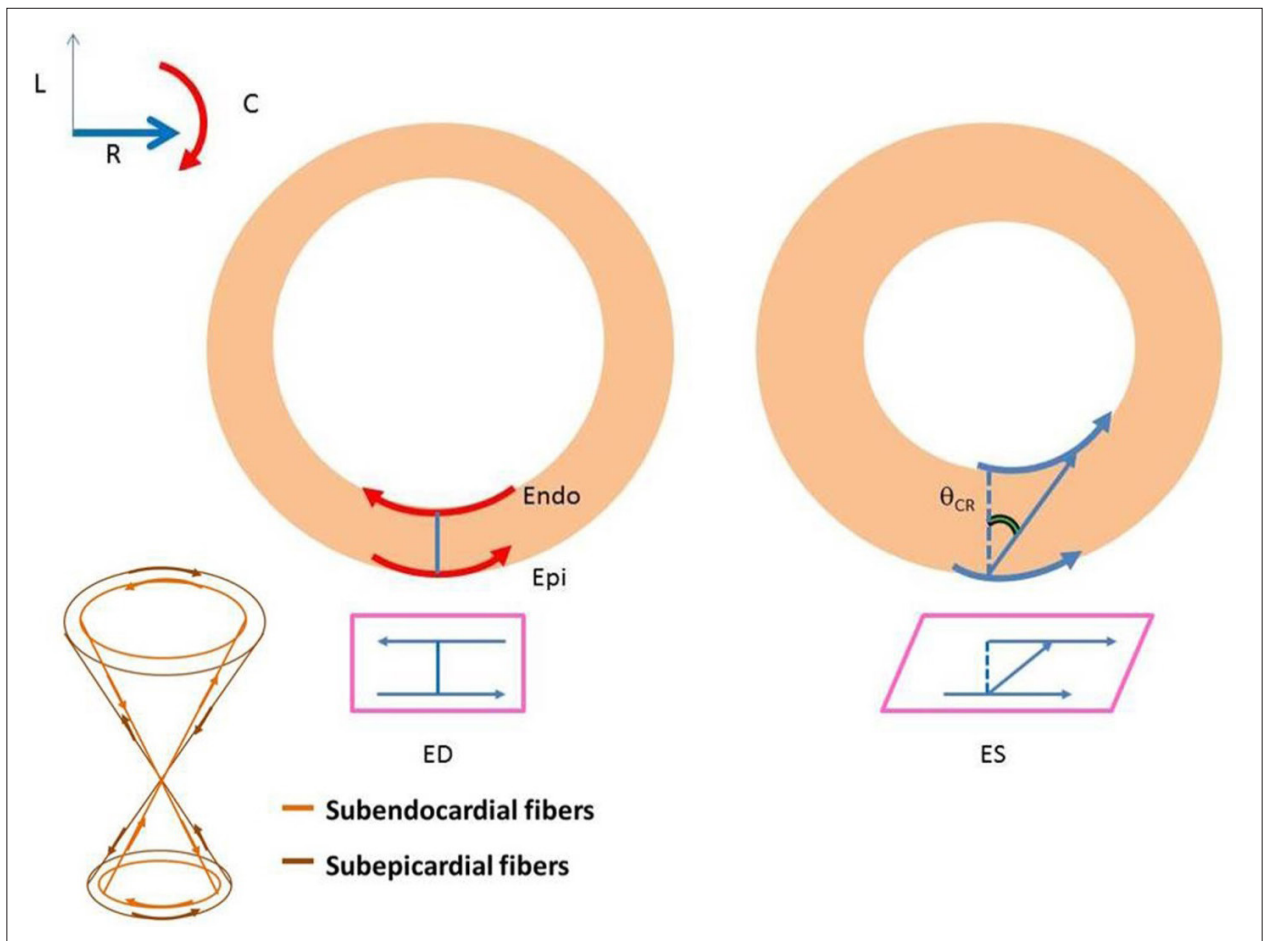


Figure 4 - Circumferential-Radial strain. Top left: as in Figure 3. Assuming that the LV apex is here represented, the subendocardial fibers are right-handed directed and the subepicardial fibers are arranged in a left-handed orientation (left and bottom left). However, due to the higher lever arm of the subepicardium, both layers slide over each other in the counterclockwise direction, resulting in CR strain (right). Red arrows: fibers orientation; blue arrows: strain direction; ED: end diastole; ES: end systole; θ_{CR} : circumferential-radial strain angle.

analysis of the ventricular function; additionally, it is not influenced by tethering^{5,1}.

Longitudinal strain seems to be the earliest to be affected by ischemia, as the subendocardial fibers are the first to suffer the effects of perfusion abnormalities¹⁹. However, Winter et al⁴⁶ showed that circumferential and radial strains are equally reduced in acute myocardial ischemia. Those authors also observed a time delay to reach peak systolic strain, mainly at the circumferential plane, which is the one related to torsion. Moreover, time-domain changes have important implications for apical recoil and diastolic function.

Global longitudinal strain may predict infarct size in patients with AMI submitted to thrombolysis or revascularization⁴⁷, and this parameter was superior to LVEF in the identification of massive infarct area (larger than 20%) when compared with MRI. Regional longitudinal strain is also related to the infarct scar size, evaluated by contrast-enhanced MRI: strain values $> -4.5\%$ indicated non-viable myocardial segments (AUC = 0.88), as, in the longitudinal plane, higher values represent lower absolute magnitude of deformation⁴⁸.

Hypertensive Heart Disease

Cardiac mechanics evaluated by STE can assess parameters that are less affected by loading conditions, such as recoil, which occurs during the isovolumic relaxation period (IVR). Takeuchi et al⁴⁹, studying patients with primary systemic hypertension, demonstrated a decreased amount and a delay in the ventricular recoil parallel to the magnitude of LV hypertrophy, resulting in an overlap between the untwisting and early ventricular diastolic filling, with impairment of the latter one. Park et al⁵⁰ observed that both torsion and recoil were significantly increased in individuals with grade 1 diastolic dysfunction, when compared with healthy volunteers and patients with grades 2 and 3 diastolic dysfunction. Other studies showed reduction in the recoil rate and in the longitudinal strain velocity that precede alterations in systolic function evaluated by global longitudinal strain and LVEF^{51,52}.

Aortic Valve Stenosis

Asymptomatic patients with severe aortic stenosis (AS) and normal LVEF showed impairment in the longitudinal strain

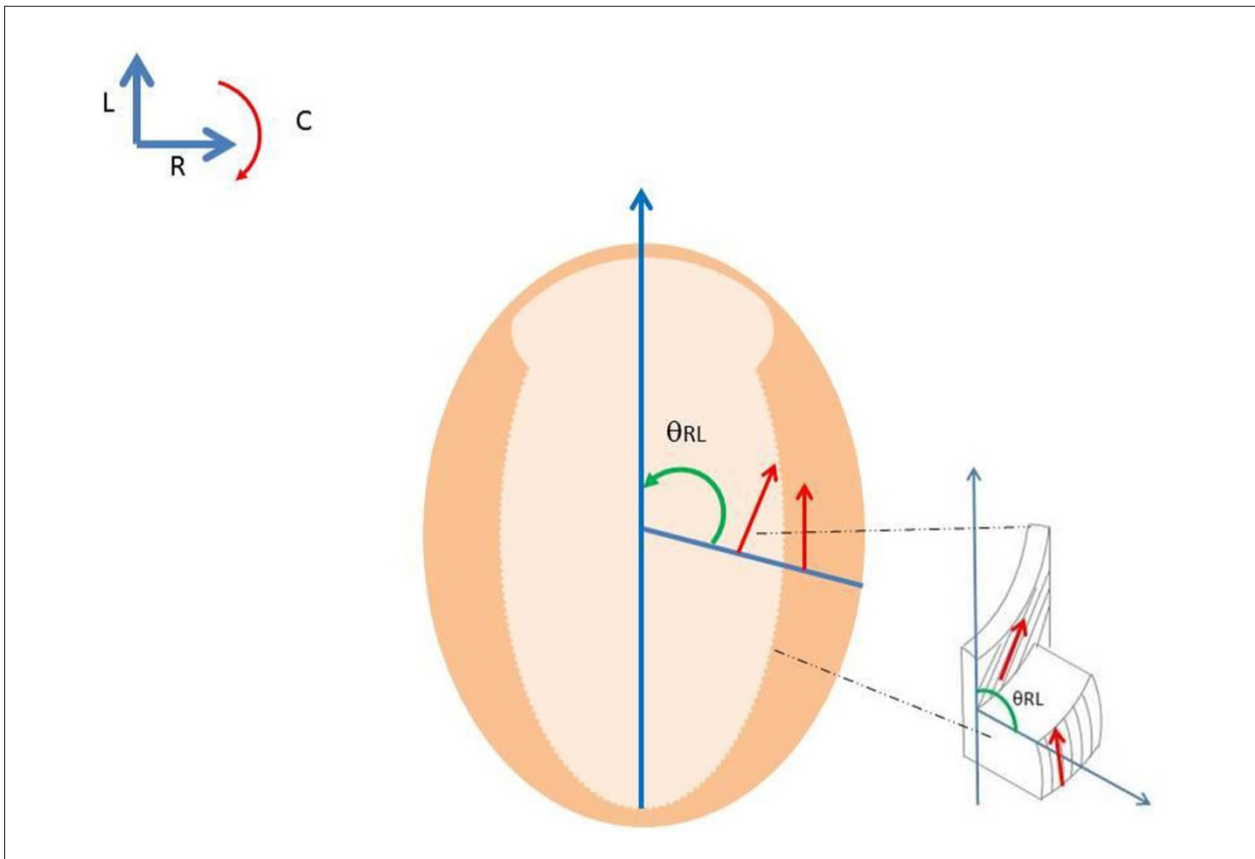


Figure 5 - Radial-Longitudinal strain. Top left: the three orthogonal planes (legends as in Figure 3). Red arrows represent the subendocardial and the subepicardial fibers orientation (right- and left-handed, respectively); the radial-longitudinal strain angle (θ_{RL} - green arrow) is originated from the sliding of the parallel planes represented by the obliquely-oriented subendo- and subepicardial layers over each other, in relation to the radial plane.

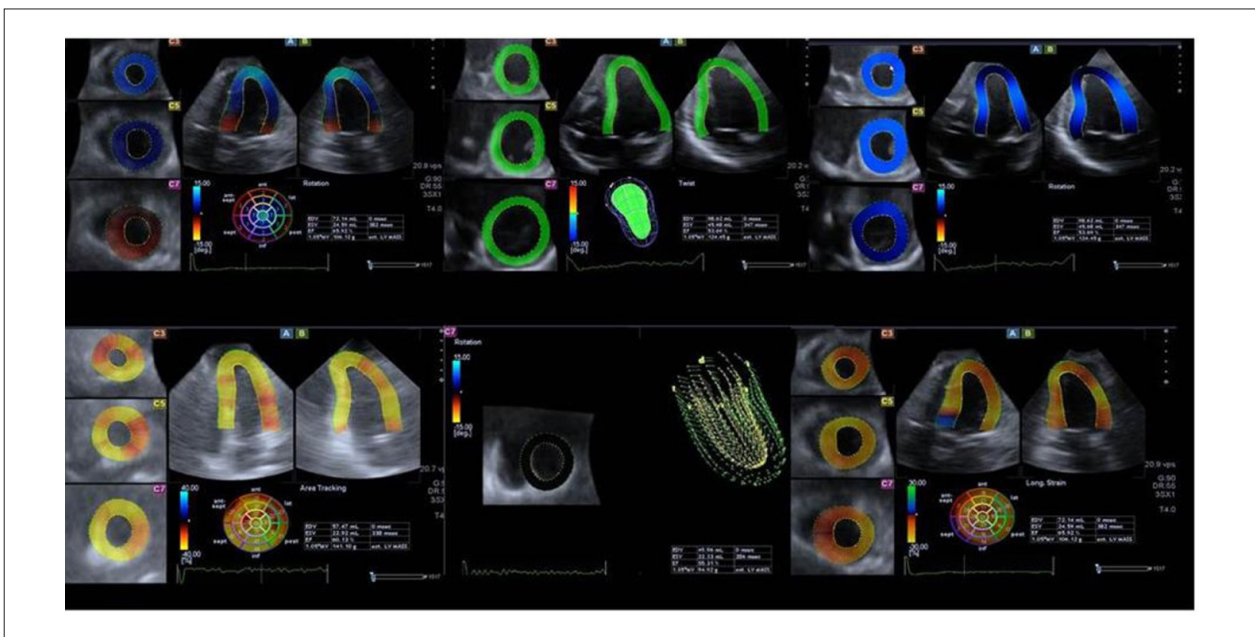


Figure 6 – Upper panel: 3D STE left ventricular analysis (volumes, ejection fraction, mass, area tracking, rotation, longitudinal strain) in a normal volunteer. **Lower panel:** 3D STE analysis (volumes, ejection fraction, mass, area tracking, rotation, longitudinal strain) in a patient with familial amyloidosis. Of note, the heterogeneity of the area tracking and longitudinal strain segments due to the amyloid deposit.

proportionally to the reduction in the valve area⁵³. Torsional mechanics was also altered in patients with moderate and severe AS: despite an increase in apical rotation, recoil was shown to be diminished, probably due to the subendocardial ischemia⁵⁴.

There is evidence of strain improvement after aortic valve replacement in patients with severe AS and normal LVEF⁵⁵. Those results indicate that LVEF may not be the most suitable diagnostic parameter to identify subtle changes in myocardial function in this population.

Mitral Regurgitation

Some studies have demonstrated reduction in LV global longitudinal strain⁵⁶ and recoil⁵⁷ in patients with moderate to severe mitral regurgitation, despite normal LVEF and dP/dt. Patients with mitral valve regurgitation may follow the same trend as those with aortic valve stenosis regarding LV systolic evaluation.

Right Ventricular Evaluation

STE adds a relevant contribution to the assessment of the right ventricle, as it is not dependent on geometrical assumptions. It enables either the identification of systolic dysfunction in patients with primary right ventricular changes, as well as in individuals presenting myocardial alterations due to the interventricular dependence^{58,59}.

Systemic Conditions that Affect the Heart

STE can be used to unmask subtle changes in the cardiac function of patients with systemic conditions, such as cancer⁶⁰ or diabetes mellitus⁶¹, as well as to differentiate between physiological and pathological hypertrophy that occurs, respectively, in athletes and in patients with storage diseases, such as Anderson-Fabry Disease⁶². This novel technology may eventually lead to new therapeutic approaches.

Limitations

As STE is based on the identification of myocardial natural markers, the adequate recognition of endocardial and epicardial borders is requested, in addition to the myocardium itself¹⁰.

References

1. Leitman M, Lysyansky P, Sidenko S, Shir V, Peleg E, Binenbaum M, et al. Two-dimensional strain - a novel software for real-time quantitative echocardiographic assessment of myocardial function. *J Am Soc Echocardiogr.* 2004;17(10):1021-9.
2. Burckhardt CB. Speckle in ultrasound B-mode scans. *IEEE Trans Sonics Ultrasonics.* 1978;25(Suppl 1):1-6.
3. D'Hooge J, Heimdal A, Jamal F, Kukulski T, Bijnens B, Rademakers F, et al. Regional strain and strain rate measurements by cardiac ultrasound: principles, implementation and limitations. *Eur J Echocardiogr.* 2000;1(3):154-70.
4. Sabbah HN, Marzilli M, Stein PD. The relative role of subendocardium and subepicardium in left ventricular mechanics. *Am J Physiol.* 1981;240(6):H920-6.
5. Reisner SA, Lysyansky P, Agmon Y, Mutlak D, Lessik J, Friedman Z. Global longitudinal strain: a novel index of left ventricular systolic function. *J Am Soc Echocardiogr.* 2004;17(6):630-3.
6. Weidemann F, Jamal F, Sutherland GR, Claus P, Kowalski M, Hatle L, et al. Myocardial function defined by strain and strain rate during alterations in inotropic states and heart rate. *Am J Physiol Heart Circ Physiol.* 2002;283(2):H792-9.
7. Dalen H, Thornstensen A, Aase SA, Ingul CB, Totrp H, Vatten J, et al. Segmental and global longitudinal strain and strain rate based on echocardiography of 1266 healthy individuals: the HUNT study in Norway. *Eur J Echocardiogr.* 2010;11(2):176-83.
8. Rüssel IK, Götte MJ, Bronzwaer JG, Knaapen P, Paulus WJ, van Rossum AC. Left ventricular torsion: an expanding role in the analysis of myocardial dysfunction. *JACC Cardiovasc Imaging.* 2009;2(5):648-55.
9. Henson RE, Song SK, Pastorek JS, Ackerman JJ, Lorenz CH. Left ventricular torsion is equal in mice and humans. *Am J Physiol Heart Circ Physiol.* 2000;278(4):H1117-23.

Moreover, in order to properly track the speckles, dedicated software requires an ideal frame rate range which, in human subjects with normal heart rate, is around 50 to 90 Hz⁶³. Values lower than these predispose to lack of information, once the algorithm is derived from the sum of absolute differences; on the other hand, an excessively elevated frame rate impairs the tracking because of speckles that practically do not move, causing mathematical instability in the algorithm⁶⁴.

Conclusions

Cardiac mechanics assessment by STE is a promising tool, considering its property of early diagnosis and prediction of events. We hypothesize that this semi-automated, noninvasive and low-cost methodology may shed light on the comprehension of the sophisticated cardiomyocyte physiology and also on the physiopathology of cardiac diseases.

Acknowledgement

To Mrs. Vanessa Pamplona from Toshiba Medical for the use of the Artida equipment, Toshiba Medical Systems.

Author contributions

Writing of the manuscript and Critical revision of the manuscript for intellectual content: Abduch MCD, Alencar AM, Mathias Jr. W, Campos Vieira MLC.

Potential Conflict of Interest

No potential conflict of interest relevant to this article was reported.

Sources of Funding

There were no external funding sources for this study.

Study Association

This study is not associated with any thesis or dissertation work.

Review Article

10. Geyer H, Caracciolo G, Abe H, Wilansky S, Carerj S, Gentile F, et al. Assessment of myocardial mechanics using speckle tracking echocardiography: fundamentals and clinical applications. *J Am Soc Echocardiogr*. 2010;23(4):351-69. Erratum in *J Am Soc Echocardiogr*. 2010;23(7):734.
11. Helle-Valle T, Crosby J, Edvardsen T, Lyseggen E, Amundsen BH, Smith HJ, et al. New noninvasive method for assessment of left ventricular rotation. *Circulation*. 2005;112(20):3149-56.
12. Notomi Y, Lysyansky P, Setser RM, Shiota T, Popovic ZB, Martin-Miklovic MG, et al. Measurement of ventricular torsion by two-dimensional ultrasound speckle tracking imaging. *J Am Coll Cardiol*. 2005;45(12):2034-41.
13. Al-Naami GH. Torsion of young hearts: a speckle tracking study of normal infants, children and adolescents. *Eur J Echocardiogr*. 2010;11(10):853-62.
14. Dong SJ, Hees PS, Huang WM, Buffer SA Jr, Weiss JL, Shapiro EP. Independent effects of preload, afterload, and contractility on left ventricular torsion. *Am J Physiol*. 1999;277(3 Pt 2):H1053-60.
15. Dong SJ, Hees PS, Siu CO, Weiss JL, Shapiro EP. MRI assessment of LV relaxation by untwisting rate: a new isovolumic phase measure of τ . *Am J Physiol Heart Circ Physiol*. 2001;281(5):H2002-9.
16. Rademakers FE, Buchalter MB, Rogers WJ, Zerhouni EA, Weisfeldt ML, Weiss JL, et al. Dissociation between left ventricular untwisting and filling. *Circulation*. 1992;85(4):1572-81.
17. Mor-Avi V, Lang RM, Badano LP, Belohlavek M, Cardim NM, Derumeaux G, et al. Current and evolving echocardiographic techniques for the quantitative evaluation of cardiac mechanics: ASE/EAE consensus statement on methodology and indications endorsed by the Japanese Society of Echocardiography. *J Am Soc Echocardiogr*. 2011;24(3):277-313.
18. Kang SJ, Lim HS, Choi BJ, Choi SY, Hwang GS, Yoon MH, et al. Longitudinal strain and torsion assessed by two-dimensional speckle tracking correlate with the serum level of tissue inhibitor of matrix metalloproteinase-1, a marker of myocardial fibrosis, in patients with hypertension. *J Am Soc Echocardiogr*. 2008;21(8):907-11.
19. Mizuguchi Y, Oishi Y, Miyoshi H, Iuchi A, Nagase N, Oki T. The functional role of longitudinal, circumferential, and radial myocardial deformation for regulating the early impairment of left ventricular contraction and relaxation in patients with cardiovascular risk factors: a study with two-dimensional strain im. *J Am Soc Echocardiogr*. 2008;21(10):1138-44.
20. Kim HK, Sohn DW, Lee SE, Choi SY, Park JS, Kim YJ, et al. Assessment of left ventricular rotation and torsion with two-dimensional speckle tracking echocardiography. *J Am Soc Echocardiogr*. 2007;20(1):45-53.
21. Jurcut R, Pappas CJ, Masci PG, Herbots L, Szulik M, Bogaert J, et al. Detection of regional myocardial dysfunction in patients with acute myocardial infarction using velocity vector imaging. *J Am Soc Echocardiogr*. 2008;21(8):879-86.
22. Saito K, Okura H, Watanabe N, Hayashida A, Obase K, Imai K, et al. Comprehensive evaluation of left ventricular strain using speckle tracking echocardiography in normal adults: comparison of three-dimensional and two-dimensional approaches. *J Am Soc Echocardiogr*. 2009;22(9):1025-30.
23. Rosen BD, Gerber BL, Edvardsen T, Castillo E, Amado LC, Nasir K, et al. Late systolic onset of regional LV relaxation demonstrated in three-dimensional space by MRI tissue tagging. *Am J Physiol Heart Circ Physiol*. 2004;287(4):H1740-6.
24. Rademakers FE, Rogers WJ, Guier WH, Hutchins GM, Siu CO, Weisfeldt ML, et al. Relation of regional cross-fiber shortening to wall thickening in the intact heart. Three-dimensional strain analysis by NMR Tagging. *Circulation*. 1994;89(3):1174-82.
25. Bogaert J, Rademakers FE. Regional nonuniformity of normal adult human left ventricle. *Am J Physiol Heart Circ Physiol*. 2001;280(2):H610-20.
26. Maffessanti F, Nesser HJ, Wienert L, Steringer-Mascherbauer R, Niel J, Gorissen W, et al. Quantitative evaluation of regional left ventricular function using three-dimensional speckle tracking echocardiography in patients with and without heart disease. *Am J Cardiol*. 2009;104(12):1755-62.
27. Seo Y, Ishizu T, Enomoto Y, Sugimori H, Aonuma K. Endocardial surface area tracking for assessment of regional LV wall deformation with 3D speckle tracking imaging. *JACC Cardiovasc Imaging*. 2011;4(4):358-65.
28. Vieira ML, Almeida MD, Ferraz Neto BH, Oliveira WA, Shoji T, Rodrigues AC, et al. Three-dimensional speckle tracking echocardiographic analysis of patients presenting familial amyloidosis. [abstract]. *J Am Soc Echocardiogr*. 2012;25(6):B79-80.
29. Ahmad H, Gayat E, Yodwut C, Abduch MC, Patel AR, Weinert L, et al. Evaluation of myocardial deformation in patients with sickle cell disease and preserved ejection fraction using three-dimensional speckle tracking echocardiography. *Echocardiography*. 2012;29(8):962-9.
30. Macron L, Lim P, Bensaïd A, Nahum J, Dussault C, Mitchell-Heggs L, et al. Single-beat versus multibeat real-time 3D echocardiography for assessing left ventricular volumes and ejection fraction. *Circ Cardiovasc Imaging*. 2010;3(4):450-5.
31. Chang SA, Lee SC, Kim EY, Hahm SH, Jang SY, Park SJ, et al. Feasibility of single-beat full-volume capture real-time three-dimensional echocardiography and auto-contouring algorithm for quantification of left ventricular volume: validation with cardiac resonance imaging. *J Am Soc Echocardiogr*. 2011;24(8):853-9.
32. Vianna-Pinton R, Moreno CA, Baxter CM, Lee KS, Tsang TS, Appleton CP, et al. Two-dimensional speckle-tracking echocardiography of the left atrium: feasibility and regional contraction and relaxation differences in normal subjects. *J Am Soc Echocardiogr*. 2009;22(3):299-305.
33. Kurt M, Wang T, Torre-Amione G, Nagueh SF. Left atrial function in diastolic heart failure. *Circ Cardiovasc Imaging*. 2009;2(1):10-5.
34. Ho SY, Sanchez-Quintana D, Cabrera JA, Anderson RH. Anatomy of the left atrium: implications for radiofrequency ablation of atrial fibrillation. *J Cardiovasc Electrophysiol*. 1999;10(11):1525-33.
35. Nahum J, Bensaïd A, Dussault C, Macron L, Clémence D, Bouhemad B, et al. Impact of longitudinal myocardial deformation on the prognosis of chronic heart failure patients. *Circ Cardiovasc Imaging*. 2010;3(3):249-56.
36. Stanton T, Leano R, Marwick TH. Prediction of all-cause mortality from global longitudinal speckle tracking: comparison with ejection fraction and wall motion scoring. *Circ Cardiovasc Imaging*. 2009;2(5):356-64.
37. Jesaityte R, Dandel M, Lehmkuhl H, Hetzer R. Prediction of short-outcomes in patients with idiopathic dilated cardiomyopathy referred for transplantation using standard echocardiography and strain imaging. *Transplant Proc*. 2009;41(1):277-80.
38. Popescu BA, Beladan CC, Calin A, Muraru D, Deleanu D, Rosca M, et al. Left ventricular remodelling and torsional dynamics in dilated cardiomyopathy: reversed apical rotation as a marker of disease severity. *Eur J Heart Fail*. 2009;11(10):945-51.
39. Afonso LC, Bernal J, Bax JJ, Abraham TP. Echocardiography in hypertrophic cardiomyopathy. The role of conventional and emerging technologies. *JACC Cardiovasc Imaging*. 2008;1(6):787-800.
40. Paraskevaidis IA, Panou F, Papadopoulos C, Farmakis D, Parissis J, Ikonomidis I, et al. Evaluation of left atrial longitudinal function in patients with hypertrophic cardiomyopathy: a tissue Doppler imaging and two-dimensional study. *Heart*. 2009;95(6):483-9.
41. van Dalen BM, Kauer F, Soliman OI, Vletter WB, Michels M, ten Cate FJ, et al. Influence of pattern of hypertrophy on left ventricular twist in hypertrophic cardiomyopathy. *Heart*. 2009;95(8):657-61.
42. van Dalen BM, Kauer F, Michels M, Soliman OI, Vletter WB, van der Zwaan HB, et al. Delayed left ventricular untwisting in hypertrophic cardiomyopathy. *J Am Soc Echocardiogr*. 2009;22(12):1320-6.
43. Popovic ZB, Kwon DH, Mishra M, Buakhamsri A, Greenberg NL, Thamilarasan M, et al. Association between regional ventricular function and myocardial fibrosis in hypertrophic cardiomyopathy assessed by speckle tracking echocardiography and delayed hyperenhancement magnetic resonance imaging. *J Am Soc Echocardiogr*. 2008;21(12):1299-305.

44. Garcia MJ, Rodriguez L, Ares M, Griffin BP, Thomas JD, Klein AL. Differentiation of constrictive pericarditis from restrictive cardiomyopathy: assessment of left ventricular diastolic velocities in longitudinal axis by Doppler tissue imaging. *J Am Coll Cardiol*. 1996;27(1):108-14.
45. Sengupta PP, Krishnamoorthy VK, Abhayaratna WP, Korinek J, Belohlavek M, Sundt TM 3rd, et al. Disparate patterns of left ventricular mechanics differentiate constrictive pericarditis from restrictive cardiomyopathy. *JACC Cardiovasc Imaging*. 2008;1(1):29-38.
46. Winter R, Jussila R, Nowak J, Brodin LA. Speckle tracking echocardiography is a sensitive tool for the detection of myocardial ischemia: a pilot study from the catheterization laboratory during percutaneous coronary intervention. *J Am Soc Echocardiogr*. 2007;20(8):974-81.
47. Sjoli B, Orn S, Greene B, Vartdal T, Smiseth OA, Edvardsen T, et al. Comparison of left ventricular ejection fraction and left ventricular global strain as determinants of infarct size in patients with acute myocardial infarction. *J Am Soc Echocardiogr*. 2009;22(11):1232-8.
48. Roes SD, Mollema SA, Lamb HJ, van der Wall EE, de Ross A, Bax JJ. Validation of echocardiographic two-dimensional speckle tracking longitudinal strain imaging for viability assessment in patients with chronic ischemic left ventricular dysfunction and comparison with contrast-enhanced magnetic resonance imaging. *Am J Cardiol*. 2009;104(3):312-7.
49. Takeuchi M, Borden WB, Nakai H, Nishikage T, Kokumai M, Nakagura T, et al. Reduced and delayed untwisting of the left ventricle in patients with hypertension and left ventricular hypertrophy: a study using two-dimensional speckle tracking imaging. *Eur Heart J*. 2007;28(22):2756-62.
50. Park SJ, Miyazaki C, Bruce CJ, Ommen S, Miller FA, Oh JK. Left ventricular torsion by two-dimensional speckle tracking echocardiography in patients with diastolic dysfunction and normal ejection fraction. *J Am Soc Echocardiogr*. 2008;21(10):1129-37.
51. Narayanan A, Aurigemma GP, Chinali M, Hill JC, Meyer TE, Tighe DA. Cardiac mechanics in mild hypertensive heart disease. *Circ Cardiovasc Imaging*. 2009;2(5):382-90.
52. Mu Y, Qin C, Wang C, Huojiaabudula G. Two-dimensional ultrasound speckle tracking imaging in evaluation of early changes in left ventricular diastolic function in patients with essential hypertension. *Echocardiography*. 2010;27(2):146-54.
53. Lafitte S, Perlant M, Reant P, Serri K, Douard H, DeMaria A, et al. Impact of impaired myocardial deformation on exercise tolerance and prognosis in patients with asymptomatic aortic stenosis. *Eur J Echocardiogr*. 2009;10(3):414-9.
54. van Dalen BM, Tzikas A, Soliman OI, Kauer F, Heuvelman HJ, Vletter WB, et al. Left ventricular twist and untwist in aortic stenosis. *Int J Cardiol*. 2011;148(3):319-24.
55. Lindqvist P, Bajraktari G, Molle R, Palmerini E, Holmgren, Mondillo S, et al. Valve replacement for aortic stenosis normalizes subendocardial function in patients with normal ejection fraction. *Eur J Echocardiogr*. 2010;11(7):608-13.
56. Borg AN, Harrison JL, Argyle RA, Ray SG. Left ventricular torsion in primary chronic mitral regurgitation. *Heart*. 2008;94(5):597-603.
57. Lancellotti P, Cosyns B, Zacharakis D, Attena E, Van Camp G, Gach O, et al. Importance of left ventricular longitudinal function and functional reserve in patients with degenerative mitral regurgitation: assessment by two-dimensional speckle tracking. *J Am Soc Echocardiogr*. 2008;21(12):1331-6.
58. Pirat B, McCulloch ML, Zoghbi WA. Evaluation of global and regional right ventricular systolic function in patients with pulmonary hypertension using a novel speckle tracking method. *Am J Cardiol*. 2006;98(5):699-704.
59. Kempny A, Diller GP, Orwat S, Kaleschke C, Kerckhoff G, Bunck ACh, et al. Right-ventricular left interaction in adults with Tetralogy of Fallot: a combined cardiac magnetic resonance and echocardiographic speckle tracking study. *Int J Cardiol*. 2012;154(3):259-64.
60. Sawaya H, Sebag IA, Plana JC, Januzzi JL, Ky B, Cohen V, et al. Early detection and prediction of cardiotoxicity in chemotherapy-treated patients. *Am J Cardiol*. 2011;107(9):1375-80.
61. Mondillo S, Cameli M, Caputo ML, Lisi M, Palmerini E, Pedelezzi M, et al. Early detection of left atrial strain abnormalities by speckle-tracking in hypertensive and diabetic patients with normal left atrial size. *J Am Soc Echocardiogr*. 2011;24(8):898-908.
62. Gruner C, Verocai F, Carasso S, Vannan MA, Jamorski M, Clarke JT, et al. Systolic myocardial mechanics in patients with Anderson-Fabry disease with and without left ventricular hypertrophy and in comparison to nonobstructive hypertrophic cardiomyopathy. *Echocardiography*. 2012;29(7):810-7.
63. Bloechlinger S, Grander W, Bryner J, Dünser MW. Left ventricular rotation: a neglected aspect of the cardiac cycle. *Intensive Care Med*. 2011;37(1):156-63.
64. Burns AT, McDonald IG, Thomas JD, MacIsaac A, Prior D, Doin´ the twist: new tools for an old concept of myocardial function. *Heart*. 2008;94(8):978-83.